8388 *Biochemistry* **2010,** *49,* 8388–8397
DOI: 10.1021/bi1005927

BIOCHEMISTRY
including biophysical chemistry & molecular biology
Article

Selective Targeting of G-Quadruplex Using Furan-Based Cyclic Homooligopeptides: Effect on c-MYC Expression[†]

Tani Agarwal,[‡] Saumya Roy,[§] Tushar Kanti Chakraborty,*[,§,∥] and Souvik Maiti*[,‡]

[‡]*Proteomics and Structural Biology Unit, Institute of Genomics and Integrative Biology, CSIR, Mall Road, New Delhi 110 007, India,* [§]*Indian Institute of Chemical Technology, CSIR, Hyderabad 500 007, India, and* [∥]*Central Drug Research Institute, CSIR, Lucknow 226 001, India*

Received April 19, 2010; Revised Manuscript Received August 16, 2010

ABSTRACT: Quadruplex-specific molecules can serve as suitable drugs in cancer therapy. We have synthesized a pair of furan-based cyclic homooligopeptides, ligand **1** and ligand **2**, to specifically target G-quadruplexes. We have shown by CD spectroscopy and UV melting that these ligands can effectively induce G-quadruplex structures in the G-rich 22-mer *c-MYC* DNA sequence and further stabilize the structure. Equilibrium binding constants measured by isothermal titration calorimeter methods indicate a high affinity of the ligands for the quadruplex structures ($K \sim 10^7$ M^{-1}) and no affinity for the duplex DNA, demonstrating that these ligands are selective for G-quadruplex structures. Surface plasmon resonance was also used to compute the binding while fluorescence resonance energy transfer-based assay was additionally used to confirm the selectivity. Moreover, using real time PCR we observed up to 90% downregulation of *c-MYC* transcripts after 24 h of ligand treatment in HeLa cells. Using a luciferase assay we show the downregulation of the protein levels. Fluorescent-assisted cell sorter-based cell cycle analysis showed a prominent arrest of cells in the sub-G1 stage upon treatment of ligands that leads toward apoptosis. Altogether, these experiments support the hypothesis that the present molecules are effective in specifically binding and stabilizing quadruplexes and provide a suitable scaffold to develop into a quadruplex-targeting therapeutic agent.

G-quadruplexes are secondary nucleic acid structures finding wide implications in various biological phenomena including gene expression and cell proliferation (*1*, *2*). Initially, G-quadruplexes were reported in the human telomeric strand and were hence rigorously probed for molecular functions like control of longevity and maintenance of cell cycle. Small molecules that bind and stabilize this structure have been demonstrated to inhibit the enzyme telomerase, which is active in 85−90% of cancer cells and inactive in normal somatic cells. G-quadruplexes have been associated with disease, due to their relative abundance in promoters of human proto-oncogenes like *c-MYC*, *c-KIT*, *c-FOS*, *KRAS*, and *c-ABL* (*3*, *4*), thereby shifting the focus of research toward their implication in therapeutics. Most studies have focused on understanding the quadruplex-mediated alteration in molecular recognition in the promoter regions and hence their bearing on disease phenotypes. It becomes rather interesting to study and develop therapeutic agents to stabilize and/or sequester these structures. In this league it has been a challenge to identify suitable ligands that can interact with G-quadruplex DNA.[1] The appropriate ligand must be highly selective for quadruplex structures and possess high specificity characterized by high binding affinity for G-quadruplexes as well as demonstrate low cytotoxicity and minimal side effects.

Despite a decade of attempts, a suitable quadruplex-targeting therapeutic agent remains to hit the market. Nevertheless, stabilization of G-quadruplexes by small molecules has recently been shown to inhibit the transcriptional activity of some oncogenes (*5*, *6*) . In their independent studies Rezler et al. (*7*) and Seenisamy et al. (*8*) have shown that diselenosapphyrin, an expanded porphyrin derivative, has 50-fold higher selectivity for quadruplex over duplex. Several ligands including derivatives of acridines (*9*), cationic porphyrin (*10*, *11*) ethidium (*12*, *13*), quindoline (*14*, *15*), and telomestatin (*16*−*19*) have been studied for their quadruplex binding ability. Most recently, hexaoxazoles (HXDV) have been developed for telomeric quadruplex targeting, with relatively good selectivity and low IC_{50} values (0.4 μM) (*20*). Recently, CX-3543, a cylene derivative and an efficient quadruplex binder, has entered phase II clinical trials (*21*). Thus, the G-quadruplex motif has emerged as a promising target for the design of selective antitumor therapeutics.

The *c-MYC* proto-oncogene whose expression is known to be controlled by a G-quadruplex motif is located in the promoter and is also implicated in various cellular processes, cell growth, proliferation, loss of differentiation, and cell death (apoptosis), and cancer development (*22*−*25*). The *c-MYC* gene is overexpressed

[†]Financial support for this work from the Council of Scientific and Industrial Research (CSIR), Government of India, and Department of Science and Technology (DST) (Swarnajanti project to S.M.), Government of India, is gratefully acknowledged. We thank CSIR for research fellowships to T.A. and S.R.

*To whom correspondence should be addressed. T.K.C.: phone, +915222623405; fax, +0915222623405; e-mail, tushar@cdri.res.in. S.M.: phone, +911127666156; fax, +9127667471; e-mail, souvik@igib.res.in.

[1]Abbreviations: CD, circular dichroism; UV, ultraviolet; ITC, isothermal titration calorimetry; FRET, fluorescence resonance energy transfer; RTPCR, real time polymerase chain reaction; NHE, nuclease hypersensitive element; FACS, fluorescence-activated cell sorting; SPR, surface plasmon resonance; PBS, phosphate-buffered saline; DNA, deoxyribonucleic acid; RNA, ribonucleic acid; 7-AAD, 7-aminoactinomycin D; T_m, melting temperature; Tmpyp4, 5,10,15,20-tetra(*N*-methyl-4-pyridyl)porphine; Se2Sap, diselenosapphyrin; TFA, trifluoroacetic acid; DMF, dimethylformamide; FDPP, pentafluorophenyldiphenylphosphinate; DMEM, Dulbeccoo's modified Eagle medium; CT DNA, calf thymus DNA.

 Published on Web 08/17/2010

Scheme 1: Structure of the G-Quadruplex Binding Ligands

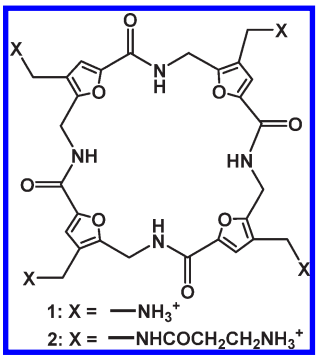

in a wide variety of human cancers, e.g., 80% of breast cancers, 70% of colon cancer, 90% of gynecological cancers, and 50% of hepatocellular carcinomas, and a variety of hematological tumors possess abnormal *c-MYC* expression. The nuclease hypersensitivity element (NHE) III_1 of the *c-MYC* promoter controls 85−90% of *c-MYC* transcription and has been the subject of considerable research over the past 2 decades. Originally identified as a major site of DNase I hypersensitivity, the NHE III_1 is located −142 to −115 bp upstream from the P1 promoter. This region being rich in guanine bases has the capability to fold into quadruplex (*23*).

Attempts at identifying suitable molecules to target G-quadruplexes have failed to combine all of the desirable features; namely, high affinity, high selectivity, and low toxicity in the same molecule have had limited success. Porphyrin being phototoxic and less selective for quadruplex is not suitable while diselenosapphyrin despite being an excellent quadruplex binder has been unsuccessful owing to low solubility in water and low yielding methods of preparation. Telomestatin finds limitation as the known strategies of its synthesis have remained inefficient. Hence new scaffolds combining these features must be identified. In an endeavor to answer this question, we developed two novel ligands based on furan amino acids (Scheme 1). In a previous study by our group, we showed that the parent molecules of the same league were efficient quadruplex binders and showed high selectivity for quadruplex over duplex (*26*). However, they showed lower binding affinities, which prompted us to modify this scaffold to display higher binding affinity. In the present study, we developed new cationic cyclic homooligopeptides, **1** and **2**, prepared from the trisubstituted furan amino acid, H-Faa-(CH_2N_3)-OH. We have employed an integrative approach to understand the behavior of these novel ligands toward quadruplex. These molecules have shown higher binding affinities while still retaining the selectivity for quadruplex. We have used CD spectroscopy, UV melting, and ITC methods to explore the binding, stabilization, and selectivity for quadruplex, along with molecular assays to understand their effect on *c-MYC* gene expression and cell survival. Additionally, through FACS we have shown the direct effect of these ligands on cell cycle perturbation and induction of apoptosis. This study has shown that the present ligands can serve as suitable molecules to selectively target quadruplexes and alter the expression of genes which possess G-quadruplex motifs in their regulatory regions.

MATERIALS AND METHODS

CD Spectroscopy. CD spectra were recorded in Jasco spectropolarimeter 50 (model 715, Japan) equipped with a thermoelectrically controlled cell holder and a cuvette with a path length of 1 cm. The oligonucleotides were heated at 95 °C for 5 min followed by slow programmed cooling (0.2 °C/min) in 10 mM Tris buffer, pH 7.4, without KCl or with 100 mM KCl. CD spectra for quadruplexes (5 μM) were recorded between 220 and 320 nm at 25 °C, and the spectra obtained were the average of three scans.

UV Melting Studies. The *c-MYC* quadruplex sample was prepared by heating the oligonucleotides in 10 mM sodium cacodylate buffer, pH 7.4, and 25 mM KCl followed by slow cooling. The melting experiment was performed with 5 μM concentration in a Cary 400 (Varian) spectrophotometer equipped with a Hitachi SPR-10 thermo programmer in the absence and presence of different molar ratios of ligands at a heating rate of 0.2 °C/min. Data were collected at 295 nm. Typically three replicate experiments were performed, and average values are reported.

FRET. 5′-Fluorescein- and 3′-dabsyl-labeled 22-mer c-myc oligonucleotide was procured from SBS Genetech. The thermal denaturation profile of the oligonucleotide at 200 nM strand concentration was recorded in the absence and presence of each of the ligands up to a quadruplex to ligand ratio of 1:8. Further in this ligand saturated system, increasing amounts of CT DNA duplex up to a base pair to ligand ratio of 100:1 were added to compete with quadruplex. FRET measurements were performed in duplicate using an LC 480 lightcycler from Roche at a heating rate of 1 °C/min. Typically three replicate experiments were performed, and average values are reported.

Isothermal Titration Calorimetry (*ITC*). ITC measurements were performed in a VP-ITC titration calorimeter (MicroCal, Northampton, MA). Before loading, the solutions were thoroughly degassed. The reference cell was filled with the degassed buffer. The preformed quadruplex (5 μM) was kept in the sample cell, and ligand (300 μM) in the same buffer was filled in the syringe of volume 300 μL. Ligand solution was added sequentially in 15 μL aliquots (for a total of 20 injections, 15 s duration each) at 5 min intervals at 25 °C. Sequential titrations were performed to ensure full occupancy of the binding sites by loading and titrating with the same ligand without removing the samples from the cell until the titration signal was essentially constant. The heats of dilution were determined in parallel experiments by injecting ligand solution of same concentration in the same buffer. The respective heats of dilution were subtracted from the corresponding binding experiments prior to curve fitting. Typically three replicate titration experiments were performed. In cases when the shape of the thermograms was nonsigmoidal due to the presence of at least two independent binding processes, the thermograms (integrated heat/injection data) obtained in ITC experiments were fit with two independent sites model.

Surface Plasmon Resonance. The following 5′-biotin-labeled oligonucleotides were procured from Sigma: c-myc, 5′-[BTN]-TTTTTTTTGGGGAGGGTGGGGAGGGTGGGG; hairpin duplex, 5′-[BTN]GCATATATATCCCCCATATATATGC. Preformed quadruplexes with these sequences in 10 mM HEPES buffer containing 25 mM KCl and 0.005% IGEPAL were immobilized onto a streptavidin-coated SA chip from Amersham. Subsequently, increasing concentrations of each of the ligands were flowed over the immobilized quadruplex, and the resulting sensorgrams were analyzed using BIAevaluation software and fitted to a 1:1 binding model to compute the binding parameters. Experiments were performed on a BIACORE 8000 system at 25 °C.

RNA Isolation and Real Time PCR. Total RNA was isolated from 1×10^6 cells using Tri-Reagent (Sigma Chemical Co.) as recommended by the manufacturer. DNase treatment was performed according to manufacturer's instructions using DNase from Invitrogen. One microgram of total RNA was reverse transcribed in a 20 μL reaction volume using an ABI high capacity cDNA reverse transcriptase kit. The cDNA was hence amplified using SYBR Green Real Time PCR Master mix from ABI in the real time PCR reactions. The amplification was done in LC 480 from Roche with the following cycling conditions for PCR: 94 °C for 2 min, followed by 35 cycles of 94 °C for 30 s, 58 °C for 30 s, and 72 °C for 30 s. Amplification of β-2 microglobulin was performed as a control using the same PCR conditions. The primers used were 5′-TGAGGAGACACCGCCCAC-3′ and 5′-CAACATCGATTTCTTCCTCATCTTC-3′ for *c-MYC* and 5′-TGCTGTCTCCATGTTTGATGTATCT-3′ and 5′-TCTCTGCTCCCCACCTCTAAGT-3′ for β-2 microglobin, respectively.

Luciferase Reporter Assay. The Del 4 plasmid (Vogelstein laboratory), which has a 22-mer c-myc quadruplex sequence cloned upstream of the luciferase promoter, was obtained as a gift. The mutant Del 4 plasmid with mutated 22-mer sequence from c-myc promoter was received from the Chowdhury laboratory as a gift. HeLa cells grown to 70% confluency in a six-well plate were transfected with 1 μg of Del 4 plasmid or mutant plasmid using Lipofectamine 2000 from Invitrogen. After 4 h, media were replaced with complete DMEM also containing increasing concentrations of ligand **2** (up to 200 μM). The expression of firefly luciferase was determined by luciferase assay (Promega); 24 h after transfection (as described by the manufacturer) cell lysate (20 μL) was mixed with 100 μL of reconstituted luciferase assay reagent, and light output was measured for 12 s with a FB12 luminometer (Berthold).

Cell Cycle Analysis. Exponentially growing HeLa cells (~45000 cells) were seeded in 12 wells and allowed to grow in DMEM complete media for 24 h. The next day cells were treated with ligand **1** and ligand **2** (0, 5, 10, 50, 100, and 200 μM) in duplicate in fresh DMEM media. After 24 h of treatment the cells were trypsinized, pelleted down, and given 1× PBS wash (twice). The cells were then resuspended in 400 μL of 70% ethanol prepared in PBS and 100 μL of 1× PBS and were stored at −20 °C overnight. For sample preparation for FACS, the samples fixed in 70% ethanol were pelleted at 6000 rpm for 5 min and then washed twice with 1× PBS. The pellet obtained was resuspended in 400 μL of 4 mM sodium citrate buffer, pH 7.4, 100 μL of 1× PBS, and 50 μL of heat-inactivated RNase (250 μg/mL), and the samples were incubated at 37 °C for 30 min. After this incubation, 10 μL of propidium iodide (5 mg/mL) was added to the samples and incubated at 4 °C for 1 h. The propidium iodide fluorescence was acquired for 5000 events using the cell cycle analysis protocol of GuavaEasycyte from Guava Technologies.

Apoptotic Cell Death Assay by FACS. Induction of apoptosis in HeLa cell line caused by ligands **1** and **2** was quantitatively determined by flow cytometry using the annexin V-conjugated 7-aminoactinomycin D (7-AAD) apoptosis detection kit (Guava Technology, Hayward, CA) following the manufacturer's instructions. Subconfluent cells (50−60%) were treated with 5, 10, 50, 100, and 200 μM concentrations of ligand **1** and **2** in 12-well plates in duplicate in complete medium for 24 h. The cells were then harvested, washed with PBS, and incubated with annexin V binding reagent added for cellular staining at room temperature for 10 min in the dark. The stained cells were analyzed by FACS using GuavaEasycyte from Guava Technologies. Nonapoptotic cells: annexin V (−) and 7-AAD (−), lower left (LL) quadrant. Early apoptotic cells: annexin V (+) and 7-AAD (−), lower right (LR) quadrant. Late stage apoptotic and dead cells: annexin V (+) and 7-AAD (+), upper right (UR) quadrant. Nuclear debris: annexin V (−) and 7-AAD (+), upper left (UL) quadrant.

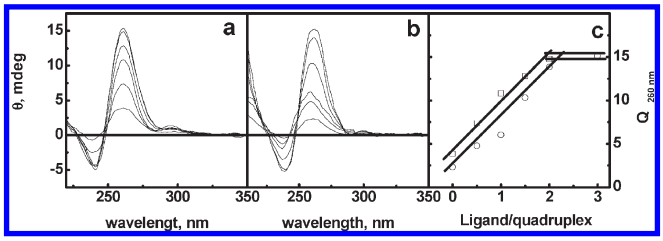

FIGURE 1: CD spectra of 5 μM c-myc 22-mer quadruplex in 10 mM Tris, pH 7.4. Spectra in the presence of 0.5, 1, 1.5, 2.0, 2.5, and 3.0 molar ratios of ligand **1** (a) and ligand **2** (b) are shown. Panel c shows CD signal at 260 nm as a function of ligand to quadruplex ratio showing an inflection point at a stoichiometry of 2.

Long-Term Viability Assay. HeLa cells were grown in 24-well plates in DMEM. Each day two wells were treated with 200 μM ligand for 6 consecutive days while two wells were replenished with fresh media without ligand to work as control samples for each day. On the last day all treated as well as control wells were processed for FACS analysis using PI staining as already mentioned, and 5000 events were acquired to get the live cell vs dead cell count.

RESULTS AND DISCUSSION

Synthesis. The syntheses of the cyclic peptides (**1**, **2**) are given in detail in the Supporting Information. The deprotected dimer TFA·H-Faa(CH_2N_3)-Faa(CH_2N_3)-OH was cyclodimerized by using pentafluorophenyldiphenylphosphinate (FDPP)[i] in DMF under dilute conditions (10^{-2} M) to give the cyclic product *cyclo*-[Faa(CH_2N_3)]$_4$ in 60% yield. Cyclic product *cyclo*-[Faa(CH_2N_3)]$_4$ could also be prepared in a single step by cyclooligomerization of the deprotected monomer TFA·H-Faa(CH_2N_3)-OH under the above conditions. But in this case we obatained *cyclo*-[Faa(CH_2N_3)]$_3$ as a major product in 30% yield with respect to *cyclo*-[Faa(CH_2N_3)]$_4$ in 11% yield. The azide groups of the cyclized product *cyclo*-[Faa(CH_2N_3)]$_4$ were reduced to primary amines by catalytic hydrogenation, followed by *in situ* protection with Boc_2O. The product was purified at the Boc-protected stage by standard silica gel column chromatography. Then Boc deprotection using TFA−CH_2Cl_2 provided the ligand **1**. Coupling of **1** with Boc-β-Ala-OH was again followed by Boc deprotection to provide the other product **2**. The final products were fully characterized by spectroscopic methods before using them in the binding studies (see Supporting Information).

Induction of Structure Monitored through Circular Dichroism Study. CD is a useful technique to observe structural transition in nucleic acids. We employed CD to evaluate the ligand-induced formation of quadruplex in the absence of any monovalent salt. The experiment was performed in two different salt conditions. In the absence of ligands, the CD spectrum of the *c-MYC* sequence was found to have a positive peak at 263 nm (Figure 1). In the presence of ligand this peak amplitude was magnified with each addition up to a ligand to quadruplex molar ratio of 2 when more ligand ceased to cause any change in the signal intensity. The change in signal at 263 nm when plotted

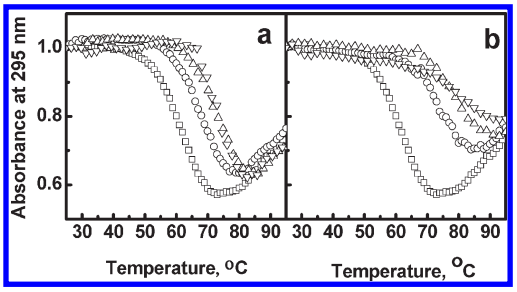

FIGURE 2: Thermal renaturation profile of the 22-mer c-myc quadruplex (5 μM) in 10 mM sodium cacodylate (25 mM KCl), pH 7.0, with no ligand (□), 5 μM ligand (○), 10 μM ligand (△), and 15 μM ligand (▽). Panel a shows melting profile with ligand **1** and panel b with ligand **2**.

against molar ratio showed saturation at a molar ratio of 2 (Figure 1c), suggesting that two ligand molecules are required for maximal folding of each DNA molecule into a G-quadruplex. To further strengthen our understanding of the induction properties of the ligands, we conducted similar experiments in the presence of 100 mM KCl also (see Supporting Information Figure 1) and found that the ligands showed no or insignificant change in the positive CD signal at 263 nm. This led us to infer that the ligands were good inducers of parallel quadruplex in the *c-MYC* 22-mer in the absence of K^+ unlike in 100 mM K^+, when the *c-MYC* 22-mer is expected to be maximally folded with high stability. At the same time it was also observed that ligands **1** and **2** caused a preferential induction of parallel topology. This quadruplex-inducing ability of the ligands impinged on the need to further assess stability of the induced structure.

UV Melting Study To Determine Thermal Stabilization. UV melting study was performed to assess the effect of ligand binding on the stability of the quadruplex structure. As ligands do not absorb themselves at 295 nm, quadruplex melting experiments were performed in the presence of 25 mM KCl and 100 mM KCl. At 100 mM KCl we observed very stable ligand quadruplex complexes such that proper melting domain could not be observed within the experimentally feasible temperature range (data not shown). Whereas at lower salt concentration, 25 mM KCl, proper melting could be seen within the observable range and the stabilizing effect of ligands could be well appreciated. Figure 2 shows the melting temperature (T_m) of the *c-MYC* quadruplex in the absence and presence of increasing amounts of ligand. The T_m of the sequence in 10 mM sodium cacodylate with 25 mM KCl in the absence of any ligand was observed to be 61 °C, while change in T_m (ΔT_m) in the presence of ligand **1** was 9, 15, and 18 °C at 1:1, 1:2, and 1:3 molar ratios, respectively. Further addition of ligand resulted in only nominal change in ΔT_m. Higher stabilization was obtained for ligand **2** leading to ΔT_m increment of 14, 20, and 25 °C at 1:1, 1:2, and 1:3 molar ratios, respectively. These ΔT_m values obtained are quite encouraging as they are in a similar range of ΔT_m reported for other well-studied quadruplex ligands like telomestatin (ΔT_m = 24 °C), the cationic porphyrin TmPyP4 (ΔT_m = 17 °C), and the other metal-based compounds like Ni(II) porphyrin (ΔT_m = 33 °C) (*27*−*29*). Since the other molecules have different geometries, they display different stoichiometries toward the *c-MYC* quadruplex (*28*, *29*).

FRET Measurements To Determine Selectivity. FRET melting has come across as a useful tool to characterize the selectivity of binding ligand toward quadruplex structure over duplex (*30*). We conducted FRET melting assay to assess the

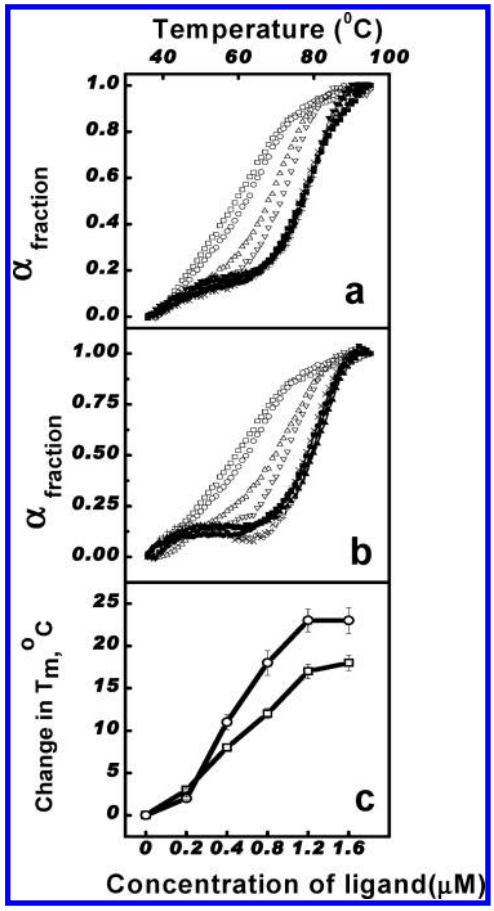

FIGURE 3: FRET melting curves show increased thermal stability of the dual-labeled 22-mer c-myc quadruplex (10 mM sodium cacodylate, pH 7.0, 25 mM KCl) in the absence and presence of ligand **1** (panel a) and ligand **2** (panel b). Scatter plots here show melting profiles in the absence of ligand (□) and with increasing quadruplex to ligand ratios: 1:1 (○), 1:2 (△), 1:4 (▽), 1:6 (×), and 1:8 (−). Further, in a 1:8 ligand-saturated system, upon addition of CT DNA (duplex) at quadruplex to duplex (CT-DNA) molar ratios 1:10 (■), 1:20 (●), 1:40 (▲), 1:60 (▼), and 1:100 (+), there was no significant change in the thermal stabilization profile indicative of high selectivity for quadruplex. Panel c shows variation of ΔT_m as a function of increasing concentration of ligand. All experiments were performed in duplicate.

thermal stabilization of fluorophore (fluorescein)−quencher (dabcyl)-tagged quadruplex in the presence of 25 mM KCl in the absence and presence of increasing amounts of ligands. The melting temperature (T_m) of the *c-MYC* quadruplex in the absence and presence of increasing amounts of ligand was analyzed by calculating the alpha fraction of the fluorescence vs temperature curves. The T_m of the sequence in 10 mM sodium cacodylate with 25 mM KCl in the absence of any ligand was observed to be 59 °C, while ΔT_m in the presence of ligand **1** was 3, 8, 12, 17, and 18 °C at 0.2, 0.4, 0.8, 1.2, and 1.6 μM ligand, respectively (Figure 3a). Further addition of ligand resulted in only nominal change in ΔT_m. Higher stabilization was obtained for ligand **2** leading to ΔT_m increment of 2, 11, 18, 23, and 23 °C at 0.2, 0.4, 0.8, 1.2, and 1.6 μM ligand, respectively (Figure 3b). These ΔT_m values obtained are quite encouraging as they are in a similar range of ΔT_m reported for other well-studied quadruplex ligands like telomestatin (ΔT_m = 24 °C), the cationic porphyrin TmPyP4 (ΔT_m = 17 °C), and the other metal-based compounds like Ni(II) porphyrin (ΔT_m = 33 °C) (*31*, *32*). The plot of ΔT_m vs molar concentration of ligand shows the gradual increase in ΔT_m

with increasing concentration of ligand in the system, thus suggesting increased binding and hence stabilization of the quadruplex (Figure 3c) .

We extended the assay to include CT DNA to understand competitive binding to duplex, too. Hence, in a ligand-saturated system (such that no more change in ΔT_m was recorded) we added increasing amounts of CT DNA. Interestingly, there was no significant change in the melting temperatures despite increasing amounts of duplex even at 100 μM CT DNA (in base pair). This is a prompt exhibition of selectivity of ligands to bind with only quadruplex structures and not to duplex.

Isothermal Titration Calorimetry Study To Assess Binding Parameters. We conducted an ITC study to understand the binding between 22-mer *c-MYC* quadruplex as well as duplex (CT DNA) with ligands **1** and **2** and also to study their selectivity over duplex. We performed the experiment both at lower (25 mM) and higher (100 mM) KCl concentration. Figure 4 shows typical integrated heat data for the mentioned titrations. The upper panel shows the microcalorimetric signal while the lower panel represents the binding curve generated by integrating the heat burst curves upon ligand injection. Intriguingly, the profiles obtained were quite different at the two different salt concentrations for both the ligands. Panels a and b in Figure 4 represent the thermograms obtained in the presence of 25 mM KCl for titrations with ligand **1** and ligand **2**, respectively. The ITC titrations of the quadruplex with ligands **1** and **2** exhibited two independent binding processes with different energetic profiles. In case of ligand **1**, there were two binding sites, one with high binding affinity of the order of 10^7 and stoichiometry of 2 and the other binding was relatively weak, of the order of 10^5, involving four ligand molecules for every one quadruplex molecule. This amounted to a total stoichiometry of 6 (Figure 4 and Table 1). Similarly, ligand **2** also showed high binding affinity and stoichiometries indicative of two-site binding. The binding affinities in this case were of the order of 10^7 and 10^5 with nominally higher magnitude over ligand **1** (Table 1). The stoichiometries were also 2 and 4, respectively, for the stronger end stacking and weaker sideward binding as was seen in the case of ligand **1**. Surprisingly, the picture was completely different in the presence of 100 mM KCl. As shown in Figure 4 (panel c), in the case of ligand **1**, there was only one type of binding with a binding affinity of the order of 10^6 and stoichiometry of 5. Similarly, for ligand **2** in the presence of 100 mM KCl (data not shown) the binding affinity was of the order of 10^6, and the stoichiometry was deduced to be 5 (Table1). With only a nominal difference in the magnitude of binding affinity, the two ligands showed a similar binding behavior.

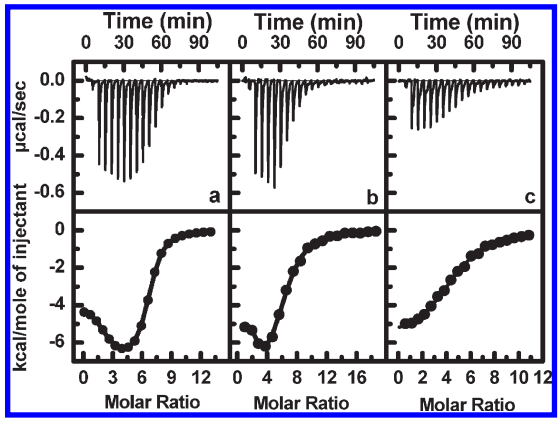

FIGURE 4: ITC thermograms showing two independent site binding in the presence of 25 mM KCl of ligand **1** (a) and ligand **2** (b) and ligand **1** in the presence of 100 mM KCl (c) with 22-mer c-myc quadruplex.

We observe in the case of both the ligands alike that the stoichiometries of interaction in 25 mM KCl as well as 100 mM KCl (5 and 6, respectively) have remained almost unaffected although binding affinities and hence binding modes have shown vast difference in the two cases. While in the case of 25 mM KCl the two bindings can be resolved into a stronger and a weaker binding as shown by the two-independent binding site curve. At higher salt concentration the binding affinity for both the modes appears to be similar such that the two binding modes are not easily distinguished once the DNA is folded maximally into quadruplex. This apparent disparity in the binding profile in different salt conditions suggests that at lower salt concentrations the ligands participate in the process of quadruplex folding, too, as is also indicated in CD results, ligands efficiently induce the structure. It has been previously observed that well-characterized quadruplex ligands like porphyrin also have similar binding profiles. In an earlier study, our group have reported porphyrin (TMPyP4) binding with four different quadruplexes. Using ITC and SPR it was shown that with *c-MYC* quadruplex there was 3:1 (porphyrin:quadruplex) binding with the two binding affinities of the order of 10^7 and 10^6, respectively. Porphyrin also showed high binding affinity with telomeric quadruplex displaying two distinct binding modes with binding affinities differing by 2 orders of magnitude (*33*). In another independent study Hurleys's group reported Se2SAP binding with 19-mer *c-MYC* quadruplex with 10^7 M^{-1} binding affinity and 1:1 stoichiometry (*34*).

From the binding isotherms we determined the thermodynamic parameters of ligand interaction using different binding mode equations. In the case of 25 mM KCl, the ΔH (enthalpy of reaction) was −5.8 kcal/mol for ligand **1**, while −1.9 kcal/mol for ligand **2**. The ΔS values were 5.72 cal mol^{-1} K^{-1} and 21.3 cal mol^{-1} K^{-1} for ligand **1** and ligand **2**, respectively. The ΔH and ΔS values of the two binding processes for both the ligands in the presence of 100 mM KCl are mentioned in Table 1. Both spectroscopic (CD as well as UV) studies and calorimetric

Table 1: Isothermal Titration Calorimetry-Derived Thermodynamic Parameters for G-Quadruplex−Ligand Interaction at 25 °C

ligand	N_1	ΔH_1 (kcal/mol)	ΔS_1 (cal mol^{-1} K^{-1})	K_1 (M^{-1})	ΔG_1 (kcal/mol)	N_2	ΔH_2 (kcal/mol)	ΔS_2 (cal mol^{-1} K^{-1})	K_2 (M^{-1})	ΔG_2 (kcal/mol)
25 mM KCl										
1	2 (±0.04)	−4.00 (±0.17)	20.22	2.40×10^7 (±0.4)	−10.02	4 (±0.05)	−7.25 (±0.08)	4.25	1.86×10^6 (±0.07)	−8.51
2	2 (±0.08)	−5.13 (±0.46)	18.70	7.71×10^7 (±0.33)	−10.71	4 (±0.12)	−8.02 (±0.2)	3.70	5.20×10^5 (±0.43)	−7.76
100 mM KCl										
1	4 (±0.05)	−5.8 (±0.01)	5.72	3.35×10^5 (±0.23)	−7.50					
2	2 (±0.42)	−1.9 (±0.1)	21.3	1.18×10^6 (±0.08)	−8.24					

(ITC) studies indicate that these ligands are efficient inducers and display promising results at lower salt concentrations.

In an attempt to establish the selectivity of these ligands toward quadruplex, it is essential to evaluate their binding with genomic (duplex) DNA. We conducted similar ITC experiments with duplex molecules using CT DNA and found that molecules showed no binding to the duplex even at low K^+ conditions (Supporting Information Figure 2). This confirmed the selectivity for quadruplex and encouraged us to further perform molecular biology assays to assess the biological consequences of *c-MYC* quadruplex and ligand interaction.

Surface Plasmon Resonance To Determine Binding Parameters. Surface plasmon resonance is a valuable technique to study DNA small molecule interactions. We used SPR to find the binding parameters of the c-MYC 22-mer quadruplex with increasing concentrations of the ligands (**1** and **2**). The representative sensorgrams are shown in Supporting Information Figure 3. Upon analysis, binding affinities were found to be 2.87 (±0.41) × 10^7 M^{-1} and 4.85 (±0.63) × 10^6 M^{-1} for ligand **1** and **2**, respectively. It was encouraging to find that the binding parameters were similar in the case of both ITC and SPR. Additionally, SPR experiments were performed with 18-mer hairpin duplex also (data not shown) to compare the strength of binding of ligands with duplex and quadruplex. But in this case, sensorgrams did not indicate any binding, and hence the data could not be properly fitted. This confirmed the absence of binding of the ligands with duplex DNA reaffirming the selectivity of the ligands for quadruplex structure.

Effect of Ligands on the Endogenous c-MYC Transcription. Next we attempted to understand the effect of quadruplex ligand interaction on transcriptional regulation of the *c-MYC* gene. Quadruplex motif in the P_1 promoter of the *c-MYC* gene has been established to have a regulatory role in *c-MYC* transcription. Therefore, we performed real time PCR to assess the transcript level of the *c-MYC* gene upon pharmacological perturbation by quadruplex binding ligands **1** and **2**. The HeLa cell line, which is an epithelial carcinoma cell line, is a well validated and widely used cell line for studying proto-oncogenes like *c-MYC*. Hence, for all cell-based assays in the study, the HeLa cell line was aptly chosen. HeLa cells were treated with 5, 10, 50, 100, and 200 μM each of the ligands **1** and **2** for 24 h each, and the total RNA was extracted, reverse transcribed into cDNA, and used as template in the real time PCR experiment. There was an evident overall decrease in the abundance of *c-MYC* transcript and was found to be downregulated with the increasing concentration of the ligands. The relative fold change was calculated by normalizing against the β-2 microglobin transcript. Figure 5 shows that in the case of **1** and **2** there was up to 80% and 90% downregulation at 200 μM ligand concentration, while 50% downregulation of *c-MYC* was observed at 50 μM ligand **1** and 10 μM ligand **2**. This reduction could result either from ligand affecting the molecular recognition of quadruplex or due to competition with transcription factors for binding site on the quadruplex. Similar results were reported by Hurley's group in their microarray study where they show that 100 μM porphyrin treatment caused downregulation of the various genes including *c-MYC* and hTERT (*35*). Also Xodo and co-workers in their study with TMPyP3 and TMPyP4 showed effective downregulation of endogenous KRAS mRNA upon treatment with 50 μM ligand. They have also shown that TmPyP2 that does not stabilize quadruplex due to its inability to stack between the G tetrads and does not reduce KRAS mRNA either (*36*). Human VEGF gene,

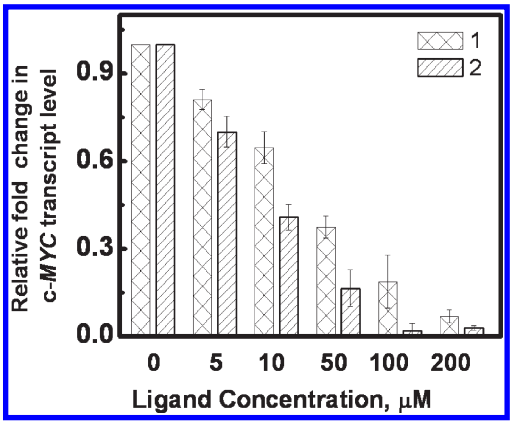

FIGURE 5: Downregulation of *c-MYC* transcripts upon treatment of ligands. RNA isolated from HeLa cells after 24 h treatment with different concentrations of ligand **1** and **2** was reverse transcribed, and real time PCR was performed. Bar charts show relative fold change in the *c-MYC* transcripts upon ligand treatment showing downregulation in a concentration-dependent manner. Normalization was done with respect to the β-2 microglobin gene. The error bars indicate standard deviation from three independent experiments.

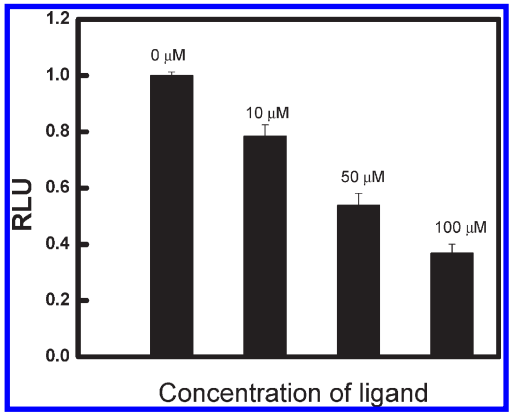

FIGURE 6: Bar charts show gradual reduction in reporter activity upon treatment of HeLa cells transfected with Del 4 plasmid (which bears the 22-mer quadruplex forming c-myc sequence upstream of the reporter) in the presence of ligand **2**. Error bars indicate standard error over three independent experiments.

which has a quadruplex motif in the proximal promoter, was shown by reverse transcriptase PCR to get downregulated in a concentration-dependent manner upon treatment with up to 50 μM TmPyP4 and Se2SAP each (*37*). In another study, Hurley and co-workers have shown 50% downregulation of firefly luciferase driven by PDGF-A promoter which reportedly harbors a G-quadruplex-forming motif subsequent to treatment with 10 μM TmPyP4 (*38*). These reports impinge on the fact that stabilization of quadruplexes in the genome can be effectively utilized to modulate gene expression.

Ligand Treatment Downregulates c-MYC Promoter Driven Reporter Expression. Having assessed the downregulation of *c-MYC* at the transcript level, we attempted to observe the effect at the protein level. For this we performed a simple luciferase reporter assay in which the plasmid containing 22-mer quadruplex forming *c-MYC* sequence cloned upstream of the firefly luciferase promoter transfected in HeLa cells showed a concentration-dependent reduction of reporter activity with ligand **2** after 24 h of treatment. Ligand **2** showed up to 60% downregulation of the promoter activity, relative to untreated samples, at 100 μM, indicating perturbance of protein levels (Figure 6). To assess the specificity of quadruplex binding, a

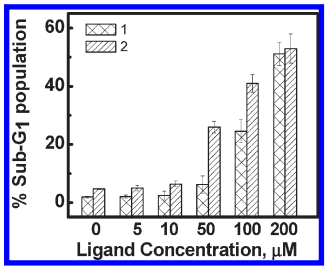

FIGURE 7: Effect of ligands on cell cycle. Bar chart shows the percentage of sub-G1 cells in HeLa cells treated for 24 h with ligands **1** and **2** at mentioned concentrations. Propidium iodide stained cells were counted by flow cytometry. The error bars indicate standard deviation from three independent experiments.

corresponding control experiment with the plasmid containing a mutated 22-mer sequence which can no longer form quadruplex was also performed. As expected, there was no significant change in reporter activity. Data have been shown in Supporting Information Figure 6. This ligand-mediated downregulation is suggestive of stabilization of the quadruplex formed by the 22mer sequence finally leading to the reduction of the reporter activity. Earlier studies have also used similar tools to confirm quadruplex binding (*39*, *40*).

Effect of c-MYC Downregulation on Cell Cycle. As cellular choice between cell growth and apoptosis is under the control of *c-MYC* stimulations and repression, we conducted further molecular assays to investigate the downstream effects of *c-MYC* suppression mediated by the quadruplex ligand interaction inside the cell. *c-MYC* finds roles in various cellular processes and plays a key function in regulating the cell cycle especially. The cell cycle is composed of four distinct phases, namely, G_1, S, G_2, and M, and is tightly regulated by the various cyclins and cyclin-dependent kinases making the progression through the various checkpoints in the different phases of cell cycle critical to cell health. The progression through these phases also marks the cell for its fate whether to divide, differentiate, or die. We wanted to investigate the effect of ligand-induced suppression of *c-MYC* on the cell cycle progression. Cells treated with different concentrations of the ligand, 5, 10, 50, 100, and 200 μM, were stained with propidium iodide and then acquired in the flow cytometer to measure the DNA content. Representative histograms depict the frequency distribution of cells in the various cell cycle phases (Supporting Information Figure 4). A typical cell cycle histogram shows cells in different phases corresponding to their DNA content. The most prominent effect was seen on the sub-G_1 cell population. As seen in Figure 7, as compared to untreated cells, there was a considerable increase in the sub-G_1 population in cells treated at the highest concentration (200 μM), 50% and 60% for ligand **1** and **2**, respectively. However, there was only moderate change in the populations of the cells in other phases. The high proportion of sub-G_1 cells was indicative of apoptotic populations and prompted us to probe the extent of apoptosis (*41*).

c-MYC Downregulation by Quadruplex-Selective Molecules Drives Cells toward Apoptosis. As already stated *c-MYC* plays major roles in the cell cycle and is also critical in apoptotic pathways in the cell. *c-MYC* is one of those key molecules that drive the cellular choice between apoptotic and metastatic pathways. Therefore, any perturbance in the levels of *c-MYC* by such targeting by quadruplex selective ligands will manifest into visible effects in the cell, pertaining to cell health and life cycle. To understand the significance of increased cell population in the sub-G1 phase, which is often the indicator of

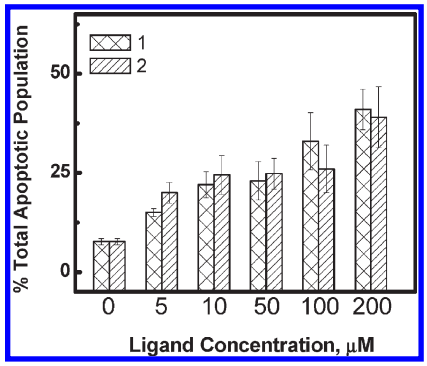

FIGURE 8: Bar graph showing the percentage of total apoptotic cells upon 24 h of ligand treatment at mentioned concentrations. Annexin V-conjugated 7-AAD nexin assay was used to count apoptotic population by flow cytometry. Error bars indicate standard error over three independent experiments.

apoptotic populations, we attempted to conduct an apoptosis assay. The assay system in our study was based on annexin V and nexin conjugated with 7-AAD. The representative dot plots displaying the frequency distribution of the cells in the four quadrants corresponding to extent of apoptosis are also shown (Supporting Information Figure 5). Figure 8 shows the bar graphs depicting the percentage of total apoptotic cells upon ligand treatment as compared to the untreated cells. In the case of ligand **1** there were almost 20% apoptotic cells at 5 μM, while at 200 μM treatment there were more than 40% cells in the same category. A similar profile with ligand **2** was seen with 20% apoptosis at 5 μM progressing up to ~38% at 200 μM. Cell cycle arrest and apoptosis induced by targeting the telomeric quadruplex with the G-quadruplex ligand pyridine in T98G glioma cells have been reported by Pennarun et al. (*42*). It is noteworthy here that, at 10 μM ligand, apoptosis is significantly increased for both ligands without much effect on cell cycle arrest. The sub-G1 population measured in the cell cycle analysis is a marker of apoptotic population. At the same time, this population may not be a direct quantitative measure of the total apoptotic population, but it certainly gives the idea of increasing or decreasing tendency toward apoptosis. Moreover, the assayed apoptotic population in the annexin V assay is additionally composed of cells which are tending to apoptosis (early in the apoptotic phase as well as late apoptotic populations) due to arrest in some stage of cell cycle like the G2/M phase or S phase.

Effect of Long-Term Ligand Treatment on Cell Viability. A long-term cell viability assay was performed to determine the cellular toxicity of both the ligands. Initially, we conducted MTT assay to determine the mitochondrial activity which is an indicator of cell viability. We observed that these ligands did not display effective inhibition of mitochondrial activity over a concentration range of 0−800 μM (data not shown). This suggested that the assay was not the appropriate indicator of cell death. Therefore, this was followed by exposure of cells to ligand for 1 week and daily assessment of live and dead populations through a sensitive FACS-based technique. At lower ligand concentrations (10 μM) we could not observe any substantial decrease in cell survival (data not shown) while at 100 μM concentration we observed a stark effect on cell viability. Figure 9 shows that markedly high cell death ensued from day 3 for both ligands **1** and **2**, resulting in 70% and 85% cell death in contrast to 25% in control. While at the end of fifth day of treatment as much as 73% and 90% cell mortality was recorded in the case of ligands **1** and **2**, respectively. The results suggest that ligands were

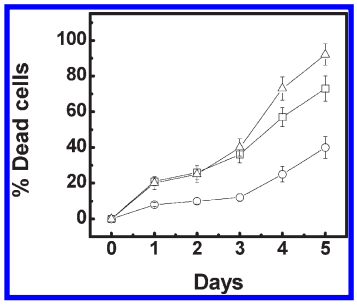

FIGURE 9: Effect of ligands on cell survival. Percentage of dead cells was measured over 5 days as compared to untreated cells (○) and after treatment with 100 μM ligand **1** (□) and **2** (△). Propidium iodide stained cells were counted using a flow cytometer and plotted as a function of days after treatment. The error bars indicate standard deviation from three independent experiments.

not cytotoxic unlike porphyrin and its cationic derivatives. The result indicates efficacious cellular response to the ligands.

Targeting quadruplex structures to modulate molecular recognition and cellular function has been an exciting field. Numerous quadruplex binding molecules have been designed, and their binding behaviors have been closely analyzed in the past. Several of these have demonstrated two binding modes. In a study from Hurley's group it was shown that porphyrin can show two distinct binding modes, an intercalative and an end stacking mode for binding to *c-MYC* 27-mer (*43*). While in a recent study, our group showed two distinct binding modes for porphyrin with quadruplex including end stacking and external binding with varying binding affinities and stoichiometry (*44*). Telomestatin is another widely investigated quadruplex ligand. The experimental data about its binding modes and binding sites are yet unavailable, but our molecular dynamics data describe it as a strong telomeric quadruplex binder with two distinct binding sites (*45*). Contextually, Hurley and co-workers in a study showed a second weaker binding mode with *c-MYC* quadruplex at higher ligand concentrations over and above a first specific binding, at the lower ligand concentrations (*46*). In our earlier reports we have also shown that porphyrin exhibits two distinct modes for binding with quadruplex with different binding affinities. The two modes of binding discussed there include end stacking and external binding (*11*). Hence, the trend of two distinct binding modes in the context of quadruplex binding is well reported. We suggest that the two binding modes observed in the present study with ligands **1** and **2** are end stacking and external binding again. The intercalative binding mode in the case of quadruplex−ligand interaction seems less feasible as has been argued by Neidle and co-workers in their crystallographic study with porphyrin (*47*). With two binding modes our ligands show two distinct binding behaviors with different binding affinities and stoichiometry. We obtained a binding affinity of the order of 10^7 and 10^6 corresponding to stronger end stacking and weaker external binding modes, respectively. Porphyrin reportedly binds with 10^7 and 10^6 M^{-1} binding affinity, and Se2SAP shows 10^6 M^{-1} binding with quadruplex. While oxazole-based molecules from Balasubramanian's group show a K_D value of 15 μM with human telomeric quadruplex as determined by SPR (*48*). In another study with oxazole derivatives HXDV and HXLV's, the ITC-derived binding affinity has been found out to be 10^5 M^{-1} (*49*). These binding affinity data confer the potential of our molecules as strong quadruplex binding ligands with binding affinities in a higher or a comparable range with other well-characterized ligands (*42*−*44*).

We also show through ITC that ligands **1** and **2** do not bind to CT-DNA (duplex) and are highly selective for quadruplex. Arguably higher selectivity than other ligands available in literature is thus demonstrated. Porphyrin binds to duplex with a 10^6 M^{-1} binding affinity (1 order less than that for quadruplex); Se2SAP binds weakly with duplex again with 10^6 M^{-1} binding affinity. Pilch and co-workers have reported selectivity of HXDV's for quadruplex over salmon testes DNA in a UV melting study (*41*), while ligands **1** and **2** in our study show absence of any heat change during ligand CT DNA interaction, indicating failure to bind with CT-DNA. The binding affinity and high selectivity have also been demonstrated in *in vivo* (cell culture) conditions. The ligands show effective suppression of *c-MYC* expression as determined in the RT-PCR experiments; 50 μM ligand **1** and 10 μM ligand **2** reduced *c-MYC* expression to 50% after 24 h treatment in HeLa cells. Porphyrin has been reported to effectively downregulate *c-MYC* at 100 μM concentration in various independent studies (*50*, *51*), while 50 μM TmPyP4 was consumed for reducing KRAS expression to 30% in pancreatic adenocarcinoma cells (*52*). Evaluation of the downstream effects of *c-MYC* suppression was done by assessing the effects on cell cycle and further on apoptosis. It was found that the ligands effectively drive the cells toward apoptosis, which may be the result of *c-MYC* downregualtion. All of these results unanimously suggest that the present ligands are highly effective quadruplex binders and can modulate the activity of the genes that bear a potential quadruplex in their regulatory element.

Structure-specific targeting of regulatory regions in the genes to influence their biological activity requires highly specific and efficient binding agents. The previously characterized quadruplex ligands have each shown some limitations. Porphyrin being highly cytotoxic and photoactive has been ruled out as a drug candidate (*52*, *53*). Se2SAP though less cytotoxic than porphyrin shows inefficient cellular uptake and hence has limited *in vivo* activity (*7*). Telomestatin has been a preferred ligand for *in vitro* quadruplex targeting but has a limitation in its poor water solubility. Though the experimental values of telomestatin are unavailable, yet studies have revealed that the oxazole moiety is the preferred scaffold for G-quadruplex-specific ligands (*40*). Several groups have designed different molecules of this league for G-quadruplex targeting (*52*, *54*−*56*), but the so far tested oxazole derivatives have shown promising biophysical properties, yet their *in vivo* activity remains to be characterized. We have shown our ligands to be highly selective and efficient quadruplex binders along with low cytotoxicity and appreciable cellular uptake in the *in vitro* as well as *in vivo* experiments. In the present study we have focused on only one representative gene, *c-MYC*, of the group of genes that bear a quadruplex motif in their regulatory elements. Further studies encompassing other members of the group along with a genome wide expression profiling shall be instrumental in establishing the selectivity of these ligands for quadruplex. It would also be challenging to investigate if the ligands can distinguish between the different (polymorphic) quadruplex structures available in the genomic scenario.

CONCLUSION

In our study we have designed and synthesized a set of molecules to be considered as potential scaffolds for selective targeting of quadruplexes. This study entails an integrative approach wherein we combine both biophysical methods and molecular assays to establish suitable scaffolds to target G-quadruplexes. In

summary, the spectroscopic and calorimetric studies have unanimously shown efficient binding, stabilization, and high selectivity for quadruplex over duplex. These ligands have proven to be promising with interesting results with molecular assays like real time PCR, reporter assay, cell-survival assay, cell cycle analysis, and apoptosis studies.

In the present study we have focused on only one representative gene, *c-MYC*, of the group of genes that bear a quadruplex motif in their regulatory elements. Further studies encompassing other members of the group along with a genome-wide expression profiling shall be instrumental in establishing the selectivity of these ligands for quadruplex. We have found that these ligands have the capability to efficiently bind with telomeric quadruplex, also (data not shown). It would also be challenging to investigate if the ligands can distinguish between the different (polymorphic) quadruplex structures available in the genomic scenario. More such studies in the future may be encouraged for better understanding of the genomic evolution as well as for applications in therapeutics.

ACKNOWLEDGMENT

We thank Prof. Bert Vogelstein for providing Del 4 which was originally gifted to Dr. Shantanu Chowdhury. We also thank Dr. Shantanu Chowdhury for gifting the Del 4 mutant plasmid.

SUPPORTING INFORMATION AVAILABLE

Experimental details for the synthesis of **1** and **2**, their spectroscopic characterization, and associated biological studies. This material is available free of charge via the Internet at http://pubs.acs.org.

REFERENCES

1. Hurley, L. H., Wheelhouse, R. T., Sun, D., Kerwin, S. M., Salazar, M., Fedoroff, O. Y., Han, F. X., Han, H., Izbicka, E., and Von Hoff, D. D. (2000) G-quadruplexes as targets for drug design. *Pharmacol. Ther. 85*, 141–158.
2. Hurley, L. H. (2001) Secondary DNA structures as molecular targets for cancer therapeutics. *Biochem. Soc. Trans. 29*, 692–696.
3. Simonsson, T. (2001) G-quadruplex DNA structures—variations on a theme. *Biol. Chem. 382*, 621–628.
4. Simonsson, T., and Henriksson, M. (2002) c-myc suppression in Burkitt's lymphoma cells. *Biochem. Biophys. Res. Commun. 290*, 11–15.
5. Siddiqui-Jain, A., Grand, C. L., Bearss, D. J., and Hurley, L. H. (2002) Direct evidence for a G-quadruplex in a promoter region and its targeting with a small molecule to repress c-MYC transcription. *Proc. Natl. Acad. Sci. U.S.A. 99*, 11593–11598.
6. Liu, W., Sun, D., and Hurley, L. H. (2005) Binding of G-quadruplex-interactive agents to distinct G-quadruplexes induces different biological effects in MiaPaCa cells. *Nucleosides, Nucleotides, Nucleic Acids. 24*, 1801–1815.
7. Rezler, E. M., Seenisamy, J., Bashyam, S., Kim, M. Y., White, E., Wilson, W. D., and Hurley, L. H. (2005) Telomestatin and diseleno sapphyrin bind selectively to two different forms of the human telomeric G-quadruplex structure. *J. Am. Chem. Soc. 127*, 9439–9447.
8. Seenisamy, J., Bashyam, S., Gokhale, V., Vankayalapati, H., Sun, D., Siddiqui-Jain, A., Streiner, N., Shin-ya, K., White, E., Wilson, W. D., and Hurley, L. H. (2005) Design and synthesis of an expanded porphyrin that has selectivity for the c-MYC G-quadruplex structure. *J. Am. Chem. Soc. 127*, 2944–2959.
9. Harrison, R. J., Cuesta, J., Chessari, G., Read, M. A., Basra, S. K., Reszka, A. P., Morrell, J., Gowan, S. M., Incles, C. M., Tanious, F. A., Wilson, W. D., Kelland, L. R., and Neidle, S. (2003) Trisubstituted acridine derivatives as potent and selective telomerase inhibitors. *J. Med. Chem. 46*, 4463–4476.
10. Han, H., Langley, D. R., Rangan, A., and Hurley, L. H. (2001) Selective interactions of cationic porphyrins with G-quadruplex structures. *J. Am. Chem. Soc. 123*, 8902–8913.
11. Kumar, N., and Maiti, S. (2005) The effect of osmolytes and small molecule on Quadruplex-WC duplex equilibrium: a fluorescence resonance energy transfer study. *Nucleic Acids Res. 33*, 6723–6732.
12. Rosu, F., De, P. E., Guittat, L., Alberti, P., Lacroix, L., Mailliet, P., Riou, J. F., and Mergny, J. L. (2003) Selective interaction of ethidium derivatives with quadruplexes: an equilibrium dialysis and electrospray ionization mass spectrometry analysis. *Biochemistry 42*, 10361–10371.
13. Breuzard, G., Millot, J. M., Riou, J. F., and Manfait, M. (2003) Selective interactions of ethidiums with G-quadruplex DNA revealed by surface-enhanced Raman scattering. *Anal. Chem. 75*, 4305–4311.
14. Zhou, J. L., Lu, Y. J., Ou, T. M., Zhou, J. M., Huang, Z. S., Zhu, X. F., Du, C. J., Bu, X. Z., Ma, L., Gu, L. Q., Li, Y. M., and Chan, A. S. (2005) Synthesis and evaluation of quindoline derivatives as G-quadruplex inducing and stabilizing ligands and potential inhibitors of telomerase. *J. Med. Chem. 48*, 7315–7321.
15. Ou, T. M., Lu, Y. J., Zhang, C., Huang, Z. S., Wang, X. D., Tan, J. H., Chen, Y., Ma, D. L., Wong, K. Y., Tang, J. C., Chan, A. S., and Gu, L. Q. (2007) Stabilization of G-quadruplex DNA and down-regulation of oncogene c-myc by quindoline derivatives. *J. Med. Chem. 50*, 1465–1474.
16. Kim, M. Y., Vankayalapati, H., Shin-ya, K., Wierzba, K., and Hurley, L. H. (2002) Telomestatin, a potent telomerase inhibitor that interacts quite specifically with the human telomeric intramolecular G-quadruplex. *J. Am. Chem. Soc. 124*, 2098–2099.
17. Rezler, E. M., Seenisamy, J., Bashyam, S., Kim, M. Y., White, E., Wilson, W. D., and Hurley, L. H. (2005) Telomestatin and diseleno sapphyrin bind selectively to two different forms of the human telomeric G-quadruplex structure. *J. Am. Chem. Soc. 127*, 9439–9447.
18. Rosu, F., Gabelica, V., Shin-ya, K., and De, P. E. (2003) Telomestatin-induced stabilization of the human telomeric DNA quadruplex monitored by electrospray mass spectrometry. *Chem. Commun. (Cambridge)*, 2702–2703.
19. Qin, Y., Fortin, J. S., Tye, D., Gleason-Guzman, M., Brooks, T. A., and Hurley, L. H. (2010) Molecular cloning of the human platelet-derived growth factor receptor beta (PDGFR-beta) promoter and drug targeting of the G-quadruplex-forming region to repress PDGFR-beta expression. *Biochemistry 49*, 4208–4219.
20. Rzuczek, S. G., Pilch, D. S., Lavoie, E. J., and Rice, J. E. (2008) Lysinyl macrocyclic hexaoxazoles: synthesis and selective G-quadruplex stabilizing properties. *Bioorg. Med. Chem. Lett. 18*, 913–917.
21. Drygin, D., Siddiqui-Jain, A., O'Brien, S., Schwaebe, M., Lin, A., Bliesath, J., Ho, C. B., Proffitt, C., Trent, K., Whitten, J. P., Lim, J. K., Von, H. D., Anderes, K., and Rice, W. G. (2009) Anticancer activity of CX-3543: a direct inhibitor of rRNA biogenesis. *Cancer Res. 69*, 7653–7661.
22. Grand, C. L., Powell, T. J., Nagle, R. B., Bearss, D. J., Tye, D., Gleason-Guzman, M., and Hurley, L. H. (2004) Mutations in the G-quadruplex silencer element and their relationship to c-MYC overexpression, NM23 repression, and therapeutic rescue. *Proc. Natl. Acad. Sci. U.S.A. 101*, 6140–6145.
23. Ma, Y., Ou, T. M., Hou, J. Q., Lu, Y. J., Tan, J. H., Gu, L. Q., and Huang, Z. S. (2008) 9-N-Substituted berberine derivatives: stabilization of G-quadruplex DNA and down-regulation of oncogene c-myc. *Bioorg. Med. Chem. 16*, 7582–7591.
24. Maiti, S., Chaudhury, N. K., and Chowdhury, S. (2003) Hoechst 33258 binds to G-quadruplex in the promoter region of human c-myc. *Biochem. Biophys. Res. Commun. 310*, 505–512.
25. Seenisamy, J., Rezler, E. M., Powell, T. J., Tye, D., Gokhale, V., Joshi, C. S., Siddiqui-Jain, A., and Hurley, L. H. (2004) The dynamic character of the G-quadruplex element in the c-MYC promoter and modification by TMPyP4. *J. Am. Chem. Soc. 126*, 8702–8709.
26. Chakraborty, T. K., Arora, A., Roy, S., Kumar, N., and Maiti, S. (2007) Furan based cyclic oligopeptides selectively target G-quadruplex. *J. Med. Chem. 50*, 5539–5542.
27. Lemarteleur, T., Gomez, D., Paterski, R., Mandine, E., Mailliet, P., and Riou, J. F. (2004) Stabilization of the c-myc gene promoter quadruplex by specific ligands' inhibitors of telomerase. *Biochem. Biophys. Res. Commun. 323*, 802–808.
28. Moorhouse, A. D., Santos, A. M., Gunaratnam, M., Moore, M., Neidle, S., and Moses, J. E. (2006) Stabilization of G-quadruplex DNA by highly selective ligands via click chemistry. *J. Am. Chem. Soc. 128*, 15972–15973.
29. Reed, J. E., Arnal, A. A., Neidle, S., and Vilar, R. (2006) Stabilization of G-quadruplex DNA and inhibition of telomerase activity by square-planar nickel(II) complexes. *J. Am. Chem. Soc. 128*, 5992–5993.
30. Tan, J. H., Gu, L. Q., and Wu, J. Y. (2008) Design of selective G-quadruplex ligands as potential anticancer agents. *Mini. Rev. Med. Chem. 8*, 1163–1178.

31. Sun, D., Thompson, B., Cathers, B. E., Salazar, M., Kerwin, S. M., Trent, J. O., Jenkins, T. C., Neidle, S., and Hurley, L. H. (1997) Inhibition of human telomerase by a G-quadruplex-interactive compound. *J. Med. Chem. 40*, 2113–2116.
32. Monchaud, D., and Teulade-Fichou, M. P. (2008) A hitchhiker's guide to G-quadruplex ligands. *Org. Biomol. Chem. 6*, 627–636.
33. Arora, A., and Maiti, S. (2008) Effect of loop orientation on quadruplex-TMPyP4 interaction. *J. Phys. Chem. B 112*, 8151–8159.
34. Shi, D.-F., Wheelhouse, R. T., Sun, D., and Hurley, L. H. (2001) Quadruplex-interactive agents as telomerase inhibitors: Synthesis of porphyrins and structure−activity relationship for the inhibition of telomerase. *J. Med. Chem., 44*, 4509–4523.
35. Grand, C. L., Han, H., Munoz, R. M., Weitman, S., Von Hoff, D. D., Hurley, L. H., and Bearss, D. J. (2002) The cationic porphyrin TMPyP4 down-regulates c-MYC and human telomerase reverse transcriptase expression and inhibits tumor growth in vivo. *Mol. Cancer Ther. 1*, 565–573.
36. Cogoi, S., Paramasivam, M., Spolaore, B., and Xodo, L. E. (2008) Structural polymorphism within a regulatory element of the human KRAS promoter: formation of G4-DNA recognized by nuclear proteins. *Nucleic Acids Res. 36*, 3765–3780.
37. Sun, D., Liu, W. J., Guo, K., Rusche, J. J., Ebbinghaus, S., Gokhale, V., and Hurley, L. H. (2008) The proximal promoter region of the human vascular endothelial growth factor gene has a G-quadruplex structure that can be targeted by G-quadruplex-interactive agents. *Mol. Cancer Ther. 7*, 880–889.
38. Qin, Y., Rezler, E. M., Gokhale, V., Sun, D., and Hurley, L. H. (2007) Characterization of the G-quadruplexes in the duplex nuclease hypersensitive element of the PDGF-A promoter and modulation of PDGF-A promoter activity by TMPyP4. *Nucleic Acids Res. 35*, 7698–7713.
39. Thakur, R. K., Kumar, P., Halder, K., Verma, A., Kar, A., Parent, J. L., Basundra, R., Kumar, A., Chowdhury, S. (2008) Metastases suppressor NM23-H2 interaction with G-quadruplex DNA within c-MYC promoter nuclease hypersensitive element induces c-MYC expression. *Nucleic Acids Res. 37*, 172−183.
40. Balkwill, G. D., Derecka, K., Garner, T. P., Hodgman, C., Flint, A. P., and Searle, M. S. (2009) Repression of translation of human estrogen receptor alpha by G-quadruplex formation. *Biochemistry 48*, 11487–11495.
41. Gajate, C., An, F., and Mollinedo, F. (2002) Differential cytostatic and apoptotic effects of ecteinascidin-743 in cancer cells. Transcription-dependent cell cycle arrest and transcription-independent JNK and mitochondrial mediated apoptosis. *J. Biol. Chem. 277*, 41580–41589.
42. Pennarun, G., Granotier, C., Gauthier, L. R., Gomez, D., Hoffschir, F., Mandine, E., Riou, J. F., Mergny, J. L., Mailliet, P., and Boussin, F. D. (2005) Apoptosis related to telomere instability and cell cycle alterations in human glioma cells treated by new highly selective G-quadruplex ligands. *Oncogene 24*, 2917–2928.
43. Freyer, M. W., Buscaglia, R., Kaplan, K., Cashman, D., Hurley, L. H., and Lewis, E. A. (2007) Biophysical studies of the c-MYC NHE III1 promoter: model quadruplex interactions with a cationic porphyrin. *Biophys. J. 92*, 2007–2015.
44. Arora, A., and Maiti, S. (2009) Stability and molecular recognition of quadruplexes with different loop length in the absence and presence of molecular crowding agents. *J. Phys. Chem. B 113*, 8784–92.
45. Agrawal, S., Ojha, R. P., and Maiti, S. (2008) Energetics of the human Tel-22 quadruplex-telomestatin interaction: a molecular dynamics study. *J. Phys. Chem. B 112*, 6828–6836.
46. Sun, D., Guo, K., Rusche, J. J., and Hurley, L. H. (2005) Facilitation of a structural transition in the polypurine/polypyrimidine tract within the proximal promoter region of the human VEGF gene by the presence of potassium and G-quadruplex-interactive agents. *Nucleic Acids Res. 33*, 6070–6080.
47. Neidle, S., and Parkinson, G. N. (2008) Quadruplex DNA crystal structures and drug design. *Biochimie 90*, 1184–1196.
48. Jantos, K., Rodriguez, R., Ladame, S., Shirude, P. S., and Balasubramanian, S. (2006) Oxazole-based peptide macrocycles: a new class of G-quadruplex binding ligands. *J. Am. Chem. Soc. 128*, 13662–13663.
49. Pilch, D. S., Barbieri, C. M., Rzuczek, S. G., Lavoie, E. J., and Rice, J. E. (2008) Targeting human telomeric G-quadruplex DNA with oxazole-containing macrocyclic compounds. *Biochimie 90*, 1233–1249.
50. Izbicka, E., Wheelhouse, R. T., Raymond, E., Davidson, K. K., Lawrence, R. A., Sun, D., Windle, B. E., Hurley, L. H., and Von Hoff, D. D. (1999) Effects of cationic porphyrins as G-quadruplex interactive agents in human tumor cells. *Cancer Res. 59*, 639–644.
51. Mikami-Terao, Y., Akiyama, M., Yuza, Y., Yanagisawa, T., Yamada, O., and Yamada, H. (2008) Antitumor activity of G-quadruplex-interactive agent TMPyP4 in K562 leukemic cells. *Cancer Lett. 261*, 226–234.
52. Cogoi, S., Paramasivan, M., Xodo, L. E., Filichev, V. V., and Pedersen, E. B. (2007) The effect of INA [(R)-1-O-(1-pyrenylmethyl)-glycerol] insertions on the structure and biological activity of a G-quadruplex from a critical KRAS G-rich sequence. *Nucleosides, Nucleotides, Nucleic Acids. 26*, 1641–1643.
53. Kerwin, S. M. (2000) G-quadruplex DNA as a target for drug design. *Curr. Pharm. Des. 6*, 441–478.
54. Tera, M., Ishizuka, H., Takagi, M., Suganuma, M., Shin-ya, K., and Nagasawa, K. (2008) Macrocyclic hexaoxazoles as sequence- and mode-selective G-quadruplex binders. *Angew. Chem., Int. Ed. Engl. 47*, 5557–5560.
55. Barbieri, C. M., Srinivasan, A. R., Rzuczek, S. G., Rice, J. E., LaVoie, E. J., and Pilch, D. S. (2007) Defining the mode, energetics and specificity with which a macrocyclic hexaoxazole binds to human telomeric G-quadruplex DNA. *Nucleic Acids Res. 35*, 3272–3286.
56. Dash, J., Shirude, P. S., and Balasubramanian, S. (2008) G-quadruplex recognition by bis-indole carboxamides. *Chem. Commun. 26*, 3055–3057.